Analysis of Post-Tensioned Hyperbolic Paraboloid Shell Roofs

by Jehangir F. Mirza*

SYNOPSIS

Governing equations for shallow, hyperbolic paraboloid (inverted umbrella) shells are stated in the form of two fourth-order partial differential equations.[1,3,4]† Boundary condition equations are developed for the case when two opposite edges are post-tensioned. The mathematical model is solved for three umbrella shells and an equivalent flat plate. Superposition is used to obtain solutions for the case when the structure is post-tensioned on all four edges. Results are presented in the form of graphs and charts to facilitate the evaluation of structural characteristics. The advantages of post-tensioning umbrella shells are demonstrated through the use of an example problem.

INTRODUCTION

The prestressing of thin shell structures such as barrels and domes has gained wide acceptance and application with the availability of literature containing analytical and experimental studies. However, current information pertaining to the prestressing of hyperbolic paraboloid (hereafter abbreviated to HP) shells is scant and inadequate.

The advantages of prestressing thin concrete shells are numerous. First, it increases the load carrying capacity of the structure by reducing tensile stresses, thereby permitting the economic design of shell roofs covering large areas, unobstructed by columns. Second, it inhibits the cracking of concrete due to shrinkage, creep and environmental influences. This results in decreased deflection and increased water-tightness of the shell. Third, it reduces the sagging of unsupported edges and thus helps maintain the geometry of the shell. This factor inhibits the propagation of bending stresses into the shell. Finally, in general, it improves the overall stability of the shell against buckling.

A shell may be prestressed over its entire surface or along the edges only. The latter technique is preferable for HP structures since, under uniform load, they generally develop low stresses in the major portion of the shell and higher stresses in the vicinity of the edges. The inverted umbrella shell, shown in Fig. 1, is a HP structure that develops tension along the edges under gravity loads. Its structural qualities and ultimate

*Assistant Professor of Civil Engineering, North Carolina State University, Raleigh, North Carolina

†Numbers refer to references at end of article.

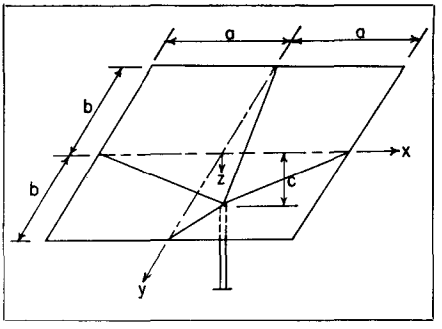

Fig. 1—Hyperbolic Paraboloid Inverted Umbrella Shell

load capacity can be considerably improved by prestressing the edges to reduce undesirable tensile stresses in the concrete.

It is the purpose of this paper to solve analytically the problem of the inverted umbrella shell with post-tensioned edges and to critically evaluate the stresses and deformation characteristics. The governing equations are expressed as two, coupled, fourth-order partial differential equations[1] in which the unknown functions are the vertical displacement component and a stress function. Boundary conditions are expressed in terms of these two functions and equations are solved by the method of finite differences. The structural characteristics of HP shells can be advantageously evaluated by comparing stresses and deformations to corresponding functions in an equivalent flat plate. Three HP shells of varying geometry and an analogous flat plate were considered. Bending moment, axial force and deformation characteristics were ascertained with the use of graphs and charts. An example problem compares structural characteristics in a uniformly loaded inverted umbrella shell with and without prestressed edges.

NOMENCLATURE, SIGN CONVENTION AND ASSUMPTIONS

The following symbols have been adopted for use in this paper:

A, B, C = arbitrary constants

a, b = horizontal dimensions of one quadrant of the shell

c = maximum vertical dimension or rise of the shell

d = bearing length over which prestressing force is uniformly distributed

D = flexural rigidity of the shell

E = modulus of elasticity in tension and compression

f = stress function

h = thickness of shell

M_x, M_y = bending moments per unit length perpendicular to the x and y axes respectively

M_{xy} = twisting moment per unit length perpendicular to the x-axis

N_x, N_y = normal forces per unit length parallel to the x and y axes respectively

$\bar{N}_x, \bar{N}_y$ = projected element forces equivalent to N_x and N_y respectively

N_{xy} = shearing force in direction of y-axis per unit length

N_{xy} = projected element force equivalent to N_{xy}

q_x, q_y, q_z = intensity of continuously distributed load components parallel to the x, y and z axes respectively

$\bar{q}_x, \bar{q}_y, \bar{q}_z$ = projected element load components equivalent to q_x, q_y and q_z respectively

T = prestressing force per unit thickness of shell

u, v, w = components of displacement parallel to the x, y and z axes respectively

V_x, V_y = Kirchoff shear force resultants on x and y faces respectively

x, y, z = cartesian shell coordinates

∇^4 = biharmonic operator

υ = Poisson's ratio

The sign convention will be as follows:

1. Vertical displacement component, w, is positive when downward.

2. Normal forces, N_x and N_y, in tension are positive.

3. Positive bending moments, M_x and M_y, create tension on the bottom or inside fibers.

4. Tangential shearing forces, N_{xy} and N_{yx}, are positive when they cause tension in the diagonal direction of increasing values of x and y.

5. Distributed load components, q_x, q_y and q_z, are positive when they act in the direction of increasing values of x, y and z.

The theoretical development is based on the following assumptions:

1. The material is linearly elastic, homogeneous and isotropic.

2. Points of the shell lying initially on a normal to the middle surface of the shell remain on this normal after deformation.

3. Displacements are small.

4. Second and higher order terms of slope components are neglected (shallow shell assumption).

GOVERNING EQUATIONS

The equation of the middle surface of the inverted umbrella shell, Fig. 1, is

$$z = \frac{c}{ab}(a-x)(b-y) \tag{1}$$

where a and b are the projected quadrant lengths parallel to the x and y axes respectively and c is the rise. The governing equations for a shallow umbrella shell are[1,4]

$$-D\nabla^4 w + \left[\frac{\partial^2 f}{\partial y^2} - \int \bar{q}_x dx\right]\frac{\partial^2 z}{\partial x^2} - 2\frac{\partial^2 f}{\partial x \partial y}\frac{\partial^2 z}{\partial x \partial y} + \left[\frac{\partial^2 f}{\partial x^2} - \int \bar{q}_y dy\right]\frac{\partial^2 z}{\partial y^2} - \bar{q}_x\frac{\partial z}{\partial x} - \bar{q}_y\frac{\partial z}{\partial y} + \bar{q}_z = 0 \tag{2}$$

$$\nabla^4 f = Eh\left[\frac{2\partial^2 z}{\partial x \partial y}\frac{\partial^2 w}{\partial x \partial y} - \frac{\partial^2 z}{\partial x^2}\frac{\partial^2 w}{\partial y^2} - \frac{\partial^2 z}{\partial y^2}\frac{\partial^2 w}{\partial x^2}\right] + \frac{\partial^2}{\partial y^2}\int \bar{q}_x dx + \frac{\partial^2}{\partial x^2}\int \bar{q}_y dy - \upsilon\left[\frac{\partial \bar{q}_y}{\partial y} + \frac{\partial \bar{q}_x}{\partial x}\right] \tag{3}$$

where

$$\nabla^4 = \text{biharmonic operator} = \frac{\partial^4}{\partial x^4} + \frac{\partial^4}{\partial x^2 \partial y^2} + \frac{\partial^4}{\partial y^4}$$

$D = Eh^3/12(1-\upsilon^2)$ = flexural rigidity of the shell

w = vertical displacement component

E = Young's modulus of elasticity

ν = Poisson's ratio
h = shell thickness
$\bar{q}_x, \bar{q}_y, \bar{q}_z$ = projected values of load intensity components parallel to the x, y and z axes respectively
f = a stress function defined as follows:

$$\frac{\partial^2 f}{\partial y^2} = \bar{N}_x + \int \bar{q}_x dx \tag{4a}$$

$$\frac{\partial^2 f}{\partial x^2} = \bar{N}_y + \int \bar{q}_y dy \tag{4b}$$

$$\frac{\partial^2 f}{\partial x \partial y} = -\bar{N}_{xy} \tag{4c}$$

$\bar{N}_x$ and $\bar{N}_y$ are projected equivalents of the actual normal forces per unit length parallel to the x and y axis respectively and $\bar{N}_{xy}$ is the shearing force per unit length in the direction of the y-axis. It is more convenient to derive the governing equations in terms of fictitious forces, such as $\bar{N}_x$ and $\bar{N}_y$, instead of their actual counterparts, N_x and N_y. (See Ref. 1 for fictitious force-actual force relationships and Ref. 5, p. 166, for more details.)

Moment-displacement equations are:

$$M_x = -D\left(\frac{\partial^2 w}{\partial x^2} + \nu \frac{\partial^2 w}{\partial y^2}\right) \tag{5a}$$

$$M_y = -D\left(\frac{\partial^2 w}{\partial y^2} + \nu \frac{\partial^2 w}{\partial x^2}\right) \tag{5b}$$

$$M_{xy} = D(1-\nu)\frac{\partial^2 w}{\partial x \partial y} \tag{5c}$$

here M_x and M_y are bending moments per unit length perpendicular to the x and y axes respectively and M_{xy} is the twisting moment per unit length perpendicular to the x-axis.

Solution of the governing equations yields expressions for the unknown variables f and w and these variables may be used to generate expressions for the force components, N_x, N_y and N_{xy}, and moment components, M_x, M_y and M_{xy}, through the application of Eqs. (4) and (5) respectively.

STATEMENT OF THE PROBLEM

If the edges of an inverted umbrella shell are post-tensioned after the concrete cures to some predetermined strength, the prestressing force would, ideally, be gradually and simultaneously applied by four jacking mechanisms at each edge. It is possible that difficulties may arise that would preclude the simultaneous use of four jacks. Under these circumstances it is probable that two opposite edges would be prestressed at one time followed by the prestressing of the other two. The forces and moments resulting from the prestressing of two opposite edges could conceivably be of critical magnitude even though the completely prestressed structure is not. It was, therefore, considered desirable to solve this latter problem and

use superposition principles to determine stresses and deformations in the completely prestressed structure. A square inverted umbrella shell with post-tensioned opposite edges, x = a and x = −a, is shown in Fig. 2. The prestressing force, T, has units of force per unit thickness of shell and is assumed uniformly distributed over the bearing length, d.

FINITE DIFFERENCE SOLUTION

In order to solve governing Eqs. (2) and (3) by the method of finite differences it is necessary to assign a numerical value to the dimensionless ratio c/h, the rise-to-thickness ratio. In HP shells this ratio generally varies between 20 and 50. Three values were chosen, viz. 24, 30 and 40. When the rise, c, is assigned the value of zero the simultaneous governing equations are uncoupled and are then the Lagrange plate equations. The case c = 0 will also be considered as a special case since the moments and deformations of an equivalent flat plate serve as an excellent datum for comparison of corresponding functions in HP shells. Poisson's ratio will be assumed equal to zero, a grid spacing equal to a/4 will be considered and the bearing length, d, of the post-tensioning force assumed equal to a/10.

To evaluate stresses in inverted umbrella shells that are not square, the governing Eqs. (1), (2) and (3) would have to be solved with rectangular dimensions a and b.

BOUNDARY CONDITIONS

The structure is axially symmetric, thus boundary conditions for only one quadrant, say the first quadrant, will be determined.

In Fig. 2, consider the edge segment y = a, $0 \leqq x \leqq (a\text{-}d)$. There are no external forces on it, thus

$$N_y = N_{xy} = 0 \qquad (6)$$

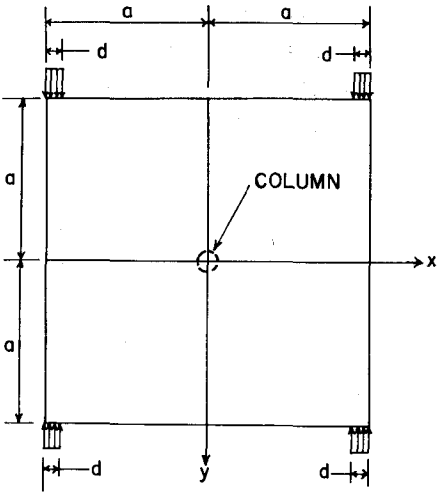

Fig. 2—Square Inverted Umbrella Shell with Opposite Edges (x = ±a) Post-Tensioned

consequently

$$\frac{\partial^2 f}{\partial x^2} = \frac{\partial^2 f}{\partial x \partial y} = 0 \qquad (7)$$

Timoshenko[2] has shown that the stress function may be taken in the form

$$f = Ax + By + C \qquad (8)$$

where A, B and C are arbitrary constants.

Taking A = B = C = 0, for the edge segment considered, the boundary conditions are

$$f = 0, 0 \leqq x \leqq (a\text{-}d) \qquad (9)$$

$$\frac{\partial f}{\partial x} = 0, 0 \leqq x \leqq (a\text{-}d) \qquad (10)$$

$$\frac{\partial f}{\partial y} = 0, 0 \leqq x \leqq (a\text{-}d) \qquad (11)$$

On the same edge consider now the segment $(a\text{-}d) \leqq x \leqq a$. Using equations of linear elasticity it can be shown[2] that

$$\frac{\partial f}{\partial x} = -\int T\,dx = -Tx + C_1 \qquad (12)$$

$$\frac{\partial f}{\partial y} = 0 \qquad (13)$$

Here T is the magnitude of the prestressing force per unit thickness of shell, and C_1 is the constant of integration. Integrating Eq. (12) yields

$$f = -\frac{T x^2}{2} + C_1 x + C_2. \quad (14)$$

The constants of integration C_1 and C_2 may be determined by requiring that the stress function and its first derivative have the same value at the junction of the two segments, i.e. at $x = (a\text{-}d)$. Equating Eqs. (10) and (12) results in

$$\left(\frac{\partial f}{\partial x}\right)_{x=a-d} = -T(a\text{-}d) + C_1 = 0$$

thus

$$C_1 = T(a\text{-}d) \quad (15)$$

Similarly, equating Eqs. (9) and (14) yields

$$(f)_{x=a-d} = -\frac{T}{2}(a\text{-}d)^2 + T(a\text{-}d)^2 + C_2 = 0$$

from which

$$C_2 = -\frac{T}{2}(a\text{-}d)^2 \quad (16)$$

Substituting Eqs. (15) and (16) in (14) and (12),

$$f = -\frac{T}{2}x^2 + T(a\text{-}d)x - \frac{T}{2}(a\text{-}d)^2, \quad (a\text{-}d) \leqq x \leqq a \quad (17)$$

$$\frac{\partial f}{\partial x} = -Tx + T(a\text{-}d), \quad (a\text{-}d) \leqq x \leqq a \quad (18)$$

$$\frac{\partial f}{\partial y} = 0, \quad 0 \leqq x \leqq a \quad (19)$$

At the corner, $y = a$, $x = a$, Eqs. (17), (18) and (19) respectively reduce to the following:

$$(f)_{x=a} = -\frac{T}{2}d^2 \quad (20)$$

$$\left(\frac{\partial f}{\partial x}\right)_{x=a} = -Td \quad (21)$$

$$\left(\frac{\partial f}{\partial y}\right)_{x=a} = 0 \quad (22)$$

The boundary $x = a$ is free of external forces; therefore, the stress function and its first derivatives would remain constant along this edge, the magnitude and the slopes being dictated by the values at the corner given in Eqs. (20), (21) and (22).

Other boundary conditions are:

$$(w)_{x=0,\,y=0} = (M_y)_{y=a} = (M_x)_{x=a} = (V_y)_{y=a} = (V_x)_{x=a} = 0 \quad (23)$$

where V_x and V_y are the Kirchoff shear force resultants on the x and y faces respectively. Internal boundary conditions along the boundaries $x = 0$ and $y = 0$ of the first quadrant are given by symmetry.

A computer program written for the IBM 1410 performed the following sequential operations:

1. Solved the non-dimensional simultaneous equations generated by the finite difference processes.
2. Dimensionalized the solution matrix.
3. Generated force and moment components.
4. Converted projected forces to actual forces.

Final moment and force components in an inverted umbrella shell are presented graphically for both conditions of prestress, viz. a) opposite edges $x = \pm a$ prestressed, and b) all four edges prestressed. Magnitudes were linearly extropolated from the values obtained by the finite difference processes. Because of axial symmetry only one quadrant is shown in most of the following diagrams. Computer results are presented in matrix form in the Appendix.

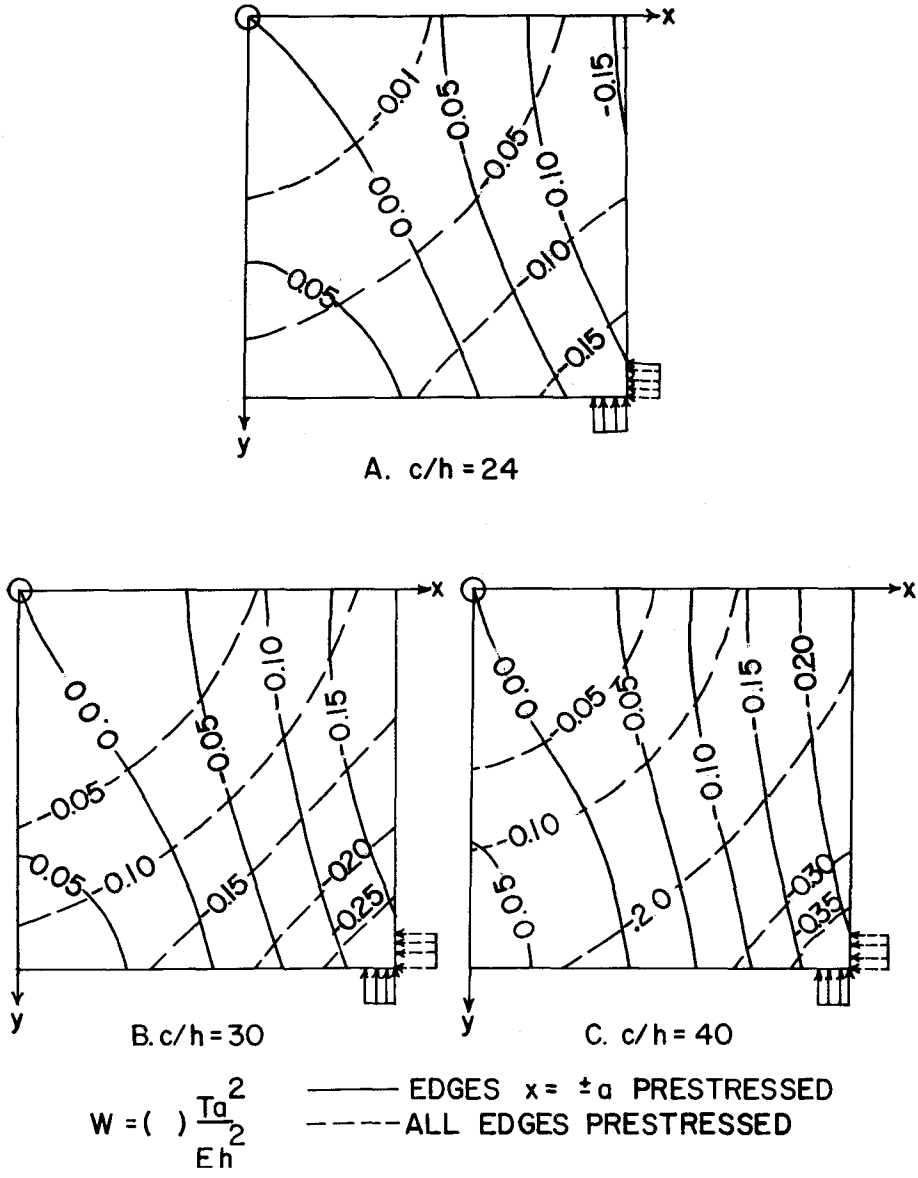

Fig. 3—Vertical Deflection Coefficient Contours

DISCUSSION OF RESULTS

Fig. 3 shows vertical displacement contours for the three inverted umbrella shells considered. The full lines represent contours for the case when edges $x = \pm a$ are prestressed and the dotted lines represent the case when all four edges are prestressed. In the former case the shell displaces vertically in such a manner that it appears to rotate about the

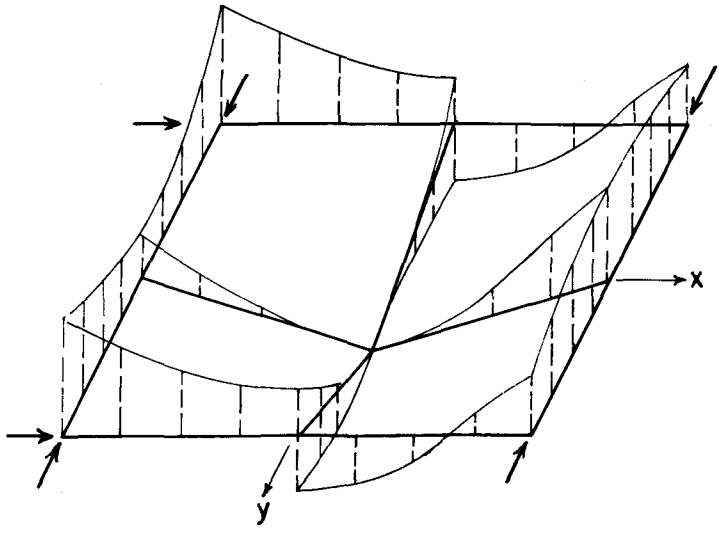

Fig. 4—Vertical Deflection Ordinates Plotted on the Surface of the Umbrella Shell for Both Stages of Prestress

zero contour. Consequently, the portion of the shell between the prestressed edge and the zero contour is displaced upwards whereas the remainder of the shell displaces downwards. This phenomena is readily discernable in Fig. 4 (right half) which is a plot of the vertical displacement ordinates on the perimeter of the shell. When all four edges are prestressed the displacement contours are diagonally symmetric (dotted lines) and indicate that the entire shell surface displaces upwards. Maximum magnitude occurs at the free corner as illustrated in Fig. 4 (left half). In Fig. 5 the variation in the vertical displacement with the rise-thickness ratio is shown to be linear. However, the extended lines do not intersect the origin indicating a nonlinear relationship as the shell rise* reduces to zero and approaches the geometry of a flat plate. This nonlinearity may be explained by the transition of structural behavior from essentially membrane to predominantly flexural as the rise diminishes to zero.

Contours for bending moments M_x (full lines) and M_y (dotted lines) are shown in Fig. 6 for the case when edges $x = \pm a$ are post-tensioned and in Fig. 7 for the case when all four edges are post-tensioned. (Bending moments, for this loading, are absent in a flat plate). The differences in contour characteristics for the two cases is not appreciably significant. However, magnitudes are somewhat higher in the former case. Bending moment profiles across significant sections are plotted in Fig. 8. The graphs indicate that M_x is approximately twice as large when only two edges are post-tensioned as compared to the case when all four edges are post-tensioned. Similarly, M_y is

**Since thin shell theory is assumed, variations in the c/h ratio are essentially due to variations in the value of c, the shell thickness, h, being relatively unvarying in magnitude.*

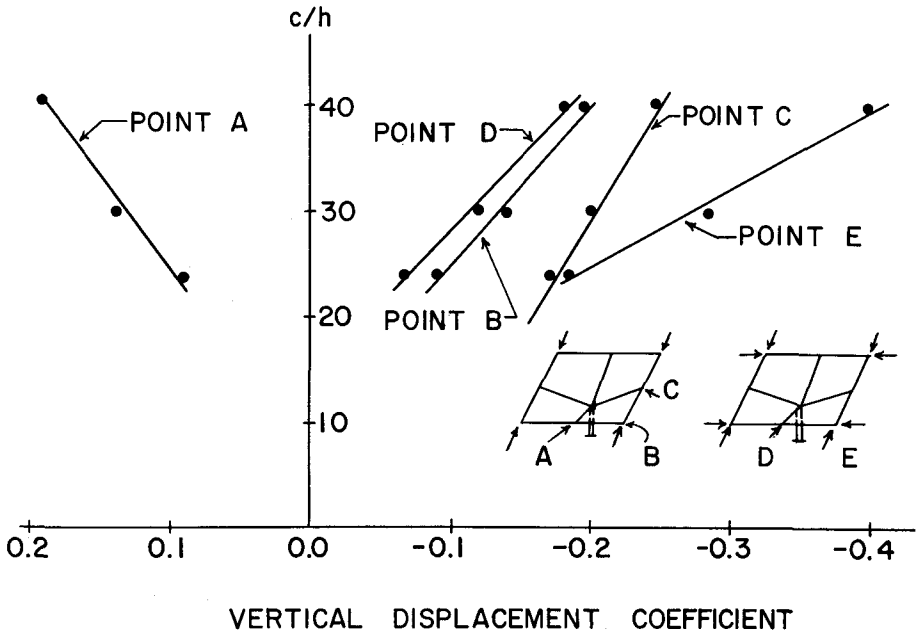

Fig. 5—Variation of the Deflection Coefficient with the Rise-Thickness Ratio

larger in the vicinity of the column support but smaller elsewhere. This indicates that bending stresses could be critical when two edges are post-tensioned even though the structure is not critical when all edges are post-tensioned. The variation of bending moments at significant points on the shell is graphed as a function of the geometry (c/h ratio) in Fig. 9. In general M_x varies inversely and M_y varies directly with the c/h ratio.

Contours for N_x (full line) and N_y (dotted line) due to post-tensioning of two edges and all four edges are plotted in Figs. 10 and 11 respectively for the three HP shells and the equivalent flat plate. The high compressive stresses originating at the edge propagate into the shell for a little over half the area when two sides are prestressed and over three-quarters of the area when all the sides are prestressed. The remainder of the shell is in tension of secondary magnitude. This fact is clearly illustrated in Fig. 12 which shows, in profile, the distribution of the normal forces across the x-axis when two opposite edges are prestressed. The local stresses in the vicinity of the bearing plate have been determined by a linear extrapolation of the finite difference results. Their accuracy is therefore questionable. This pattern of distribution of normal forces due to prestress is desirable since normal forces due to gravity loads are tensile in the vicinity of the edge and compressive elsewhere.

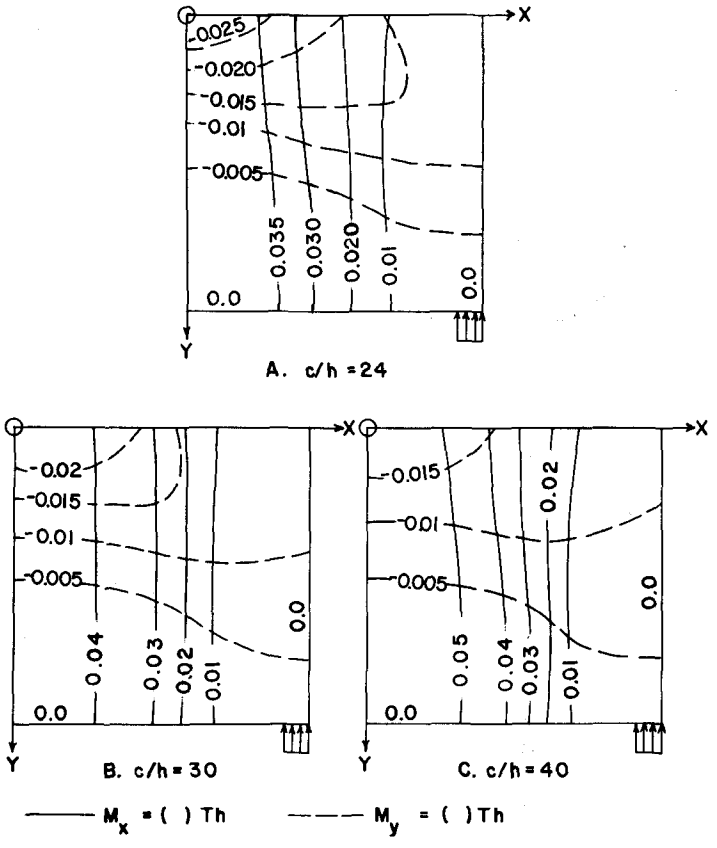

Fig. 6—Contours of Bending Moment Coefficients When Two Opposite Edges are Prestressed

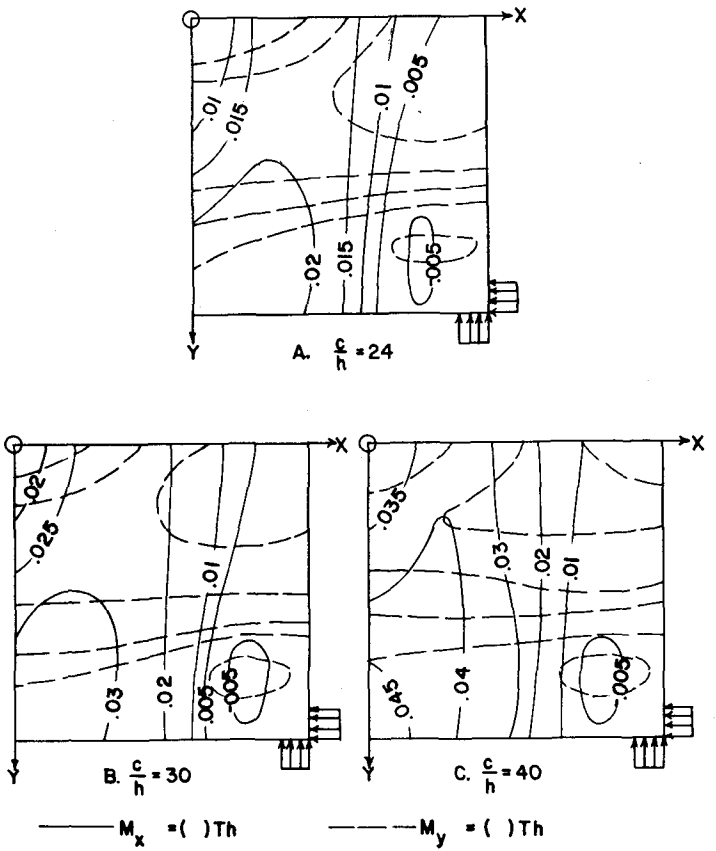

Fig. 7—Contours of Bending Moment Coefficients When All Four Sides are Prestressed

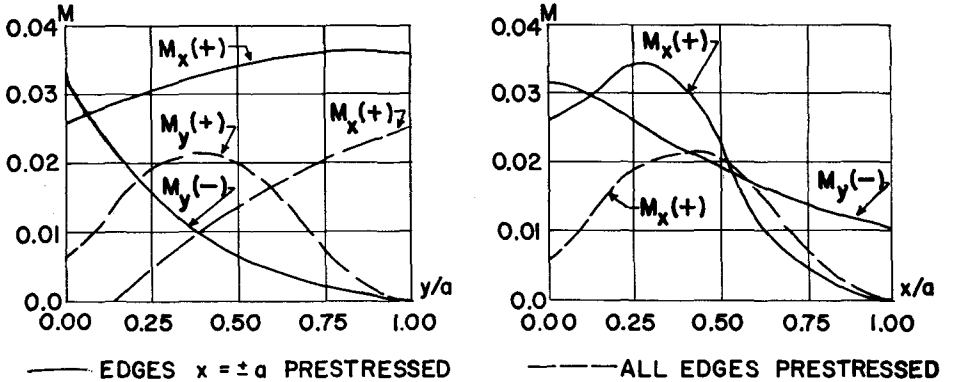

Fig. 8—Bending Moment Coefficient Profiles Across Sections Coincident with the x-Axis (right) and y-Axis (left)

SUPERPOSITION OF GRAVITY AND PRESTRESSING FORCE EFFECTS

Net moments and forces in an inverted umbrella shell subjected to both a uniformly distributed vertical load and prestressing forces on all four edges may be obtained by the superposition (i.e. the algebraic addition) of corresponding functions as obtained for each load case separately.* The principle of superposition is applicable here consistent with the stated assumptions. However, the question that now arises is: According to what criteria should the magnitude of the prestressing force be determined? The answer to this question would have to depend on each individual case. In general, however, it might be stated that the optimum prestressing force should be of sufficient magnitude so as to reduce the major tensile stresses without causing other undesirable effects.

As an example consider an inverted umbrella shell of the following dimensions: a = 12 ft., c = 4 ft., h = 2 in., E = 4×10^6 psi. The structure is subjected to a uniformly distributed vertical load of 50 psf (total

Structural characteristics of HP shells under gravity loads are evaluated and discussed in Ref. 1.

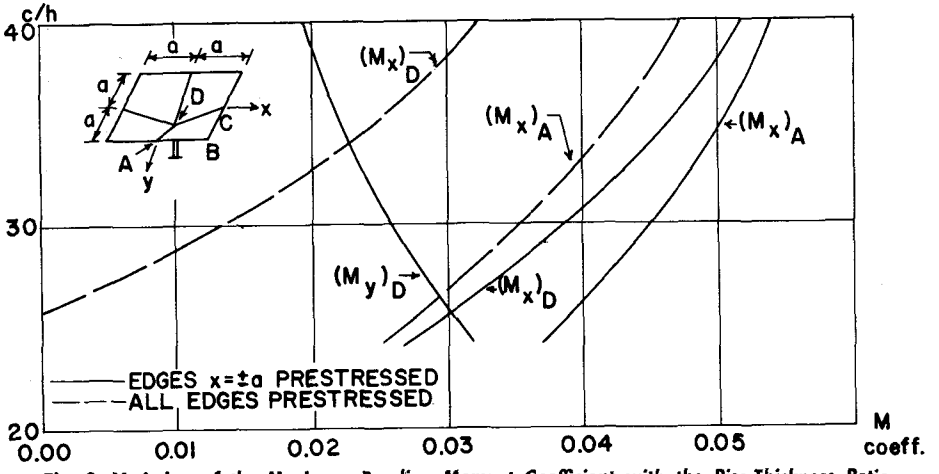

Fig. 9—Variation of the Maximum Bending Moment Coefficient with the Rise-Thickness Ratio

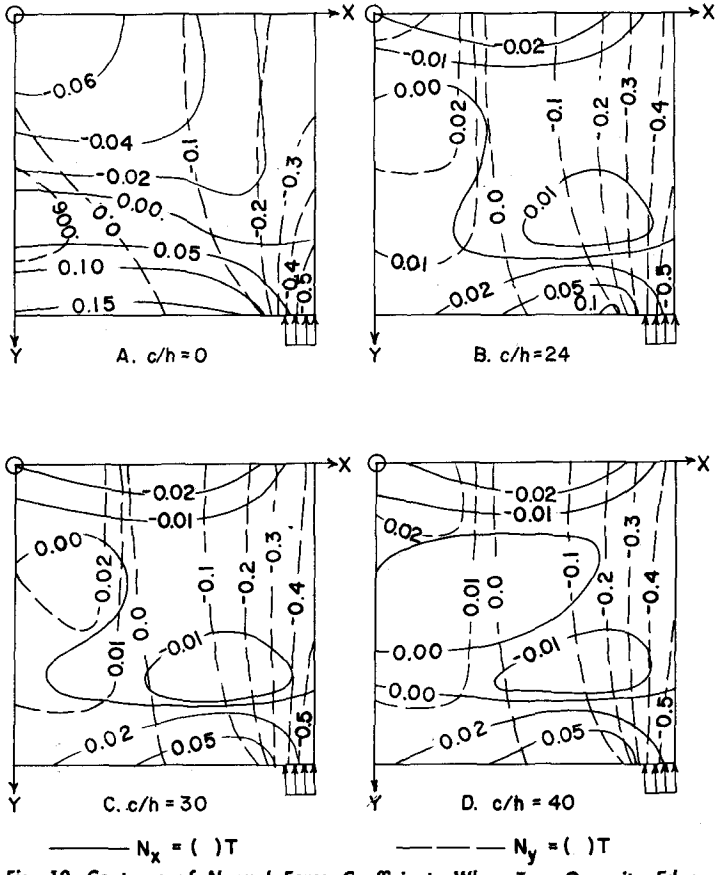

Fig. 10—Contours of Normal Force Coefficients When Two Opposite Edges are Prestressed

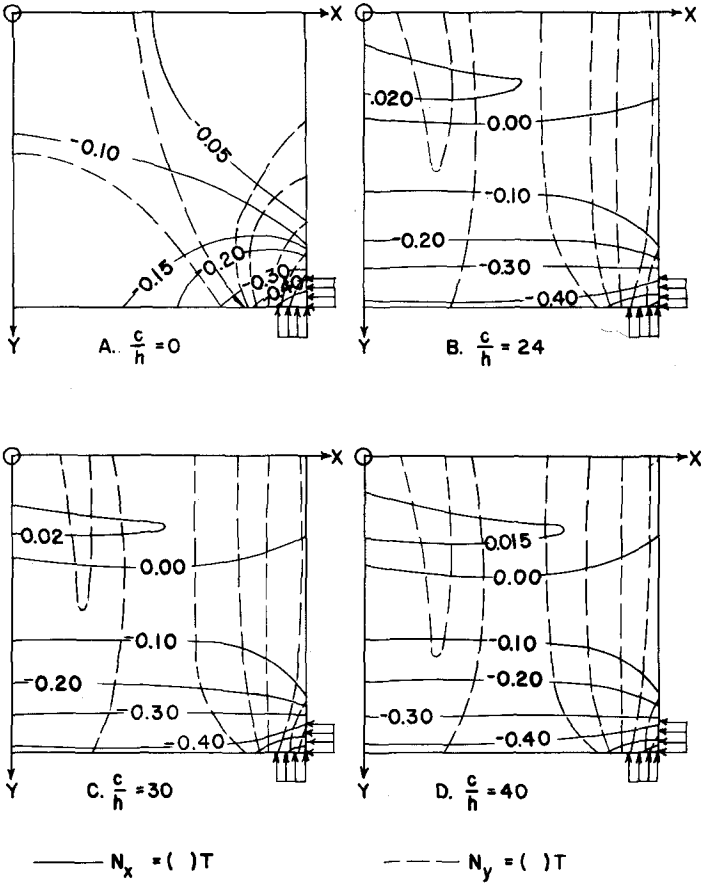

Fig. 11—Contours of Normal Force Coefficients When All Four Edges are Prestressed

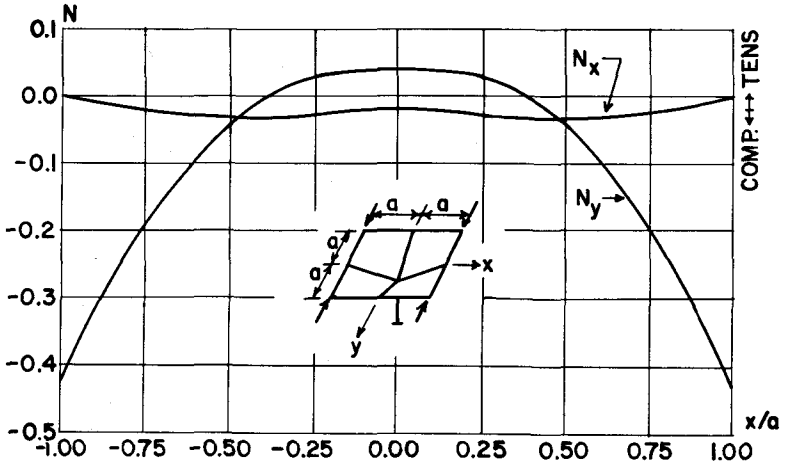

Fig. 12—Normal Force Coefficient Profiles Across a Section Coincident with the x-Axis When Two Opposite Edges are Prestressed

dead load + live load), i.e. $q_z = 50$ psf. A prestressing force of intensity $T = 6000$ lb./in., applied over a bearing length of 1.2 ft. (1/10 of the side dimension, as assumed in the derivation of equations), should be sufficient to eliminate tensile stresses without exceeding the bearing stress. The force and moment matrices are evaluated with the given data for both gravity loading and prestressing force and added. For comparative ease the resulting functional contours are presented in pairs; one for the inverted umbrella subjected to a uniformly distributed vertical load only and the other to include the superimposed prestressing force. This is shown in Figs. 13 and 14. It is noted that the corner deflection is reduced from 2.04 in. before prestressing to 0.63 in. after prestressing. Similarly the undesirable tensile stresses in the areas near the edges are eliminated and replaced by moderate compressive stresses over the majority of the shell surface. Bending moments and shearing forces are not affected to any appreciable extent.

CONCLUSIONS

1. The governing equations of an inverted umbrella shell, expressed as a pair of simultaneous, fourth-order partial differential equations, and modified by post-tensioning loads along the edges are readily solved by the method of finite differences. The results are of reasonable magnitude and their variation with geometric parameters is continuous and generally almost linear. However, nonlinear variation is expected for decreasing values of the shell rise-to-span ratio as the conditions of a flat plate are approached.

2. The prestressing of two opposite edges causes portions of the shell to displace upwards and other portions to displace downwards. When all four edges are prestressed, however, the entire surface displaces upwards. This latter effect is highly desirable to offset corner sag due to gravity loads.

3. When only two edges are prestressed, bending moments tend to be almost twice as large compared to the case when all four edges are prestressed. Thus, this intermediate

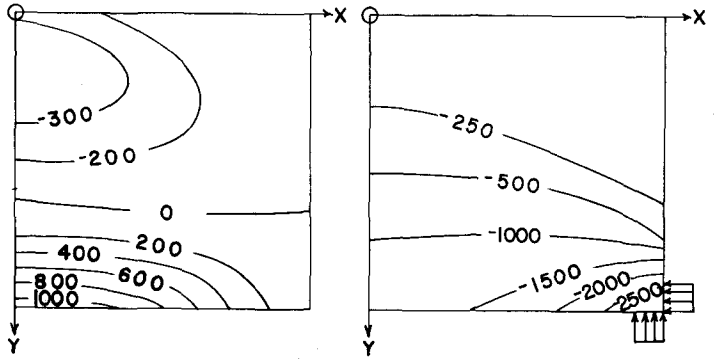

A. NORMAL FORCE, N_x (lb/in), BEFORE PRESTRESSING

B. NORMAL FORCE, N_x (lb/in), AFTER PRESTRESSING

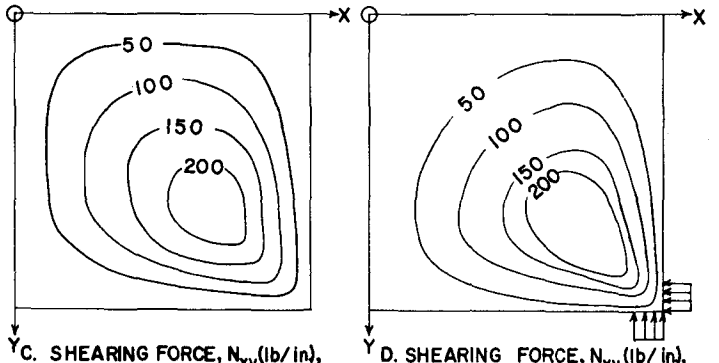

C. SHEARING FORCE, N_{xy} (lb/in), BEFORE PRESTRESSING

D. SHEARING FORCE, N_{xy} (lb/in), AFTER PRESTRESSING

Fig. 13—Contours Comparing Normal and Shearing Force Due to a Uniformly Distributed Load, Before and After Prestressing

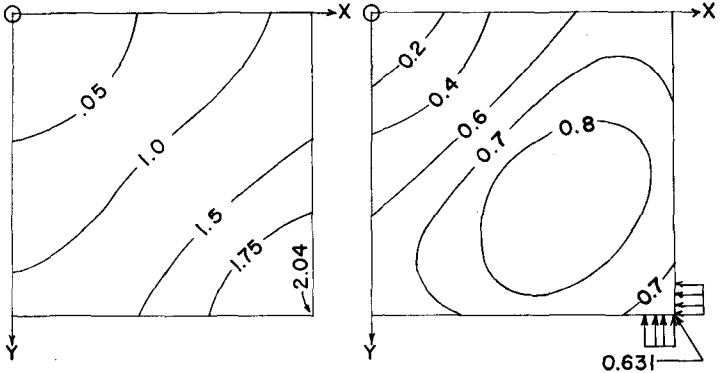

A. VERTICAL DISPLACEMENT BEFORE PRESTRESSING (inches)

B. VERTICAL DISPLACEMENT AFTER PRESTRESSING (inches)

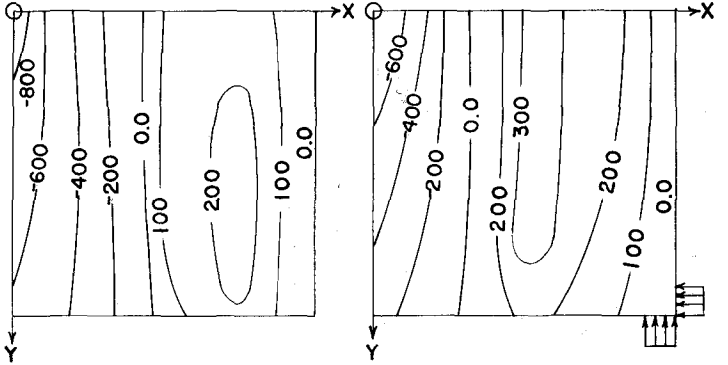

C. BENDING MOMENT, M_x, BEFORE PRESTRESSING (in.-lb/in.)

D. BENDING MOMENT, M_x, AFTER PRESTRESSING (in.-lb/in.)

Fig. 14—Contours Comparing Vertical Deflection and Bending Moment Due to a Uniformly Distributed Load, Before and After Prestressing

stage in a two-stage prestressing technique is a potentially critical one. The example problem illustrates that the prestressing of all four edges does not appreciably alter the magnitude of bending moments, present in an umbrella shell, due to gravity loads.

4. The high compressive axial force originating along the post-tensioned edges propagates into the shell for a little over half the quadrant length. The remainder of the shell is in tension.

5. Finally, it is concluded that prestressing is imperative for the economic design of large span umbrella shells. The criteria for determining the magnitude of the prestressing force would depend on each separate circumstance; however, it is more than likely to be the nullification or reduction of the edge tension.

ACKNOWLEDGMENTS

The writer wishes to thank Prof. M. E. Uyanik, the Computer Center at North Carolina State University and the Ford Foundation for assistance rendered towards the writing of this paper. Acknowledgment is also due to the National Science Foundation for research grant GK-926 to continue research in this area. Some of the material presented herein formed a portion of a doctoral dissertation[1] presented to North Carolina State University in May, 1965.

REFERENCES

1. Mirza, J. F., "A Study of the Stresses and Deformations in Shallow, Prestressed Hyperbolic Paraboloid Shells." PhD dissertation, North Carolina State Univ., 1965.
2. Timoshenko, S. P. and Goodier, J. N., "Theory of Elasticity," 1951, McGraw-Hill Book Co., New York.
3. Marguerre, K., "Zur Theorie der Gekrummten Platte grosser Formanderung," *Proceedings,* 5th International Congress of Applied Mechanics, 1938.
4. Reissner, E., "On Some Aspects of the Theory of Thin Elastic Shells," *Journal of the Boston Society of Civil Engineers,* Boston, Mass., April 1955.
5. Flugge, W., "Stresses in Shells," 1962, Springer-Verlag, Berlin, Germany.

APPENDIX

Finite difference results can be presented most conveniently in matrix format. Accordingly, the magnitude of a function at a particular node point on the finite difference grid is given by the matrix element in the corresponding position.

CASE 1. TWO OPPOSITE EDGES PRESTRESSED

Since the shell is axially symmetric, the finite difference results corresponding to the first quadrant of the umbrella prestressed on two opposite edges are given below.

Flat Plate: $c/h = 0$

$$(f) = \begin{bmatrix} .021134 & .020934 & .019173 & .012337 & -.004999 \\ .018872 & .018806 & .017523 & .011559 & -.004999 \\ .012707 & .012918 & .012735 & .009111 & -.004999 \\ .004872 & .005168 & .005740 & .004846 & -.004999 \\ .000000 & .000000 & .000000 & .000000 & -.004999 \end{bmatrix} Ta^2$$

$$(N_x) = \begin{bmatrix} -.072389 & -.068076 & -.052821 & -.024903 & .000000 \\ -.062443 & -.060182 & -.050199 & -.026714 & .000000 \\ -.026708 & -.029768 & -.035307 & -.029079 & .000000 \\ .047378 & .041289 & .020074 & -.009292 & .000000 \\ .155935 & .165400 & .183686 & .155077 & .000000 \end{bmatrix} T$$

$$(N_y) = \begin{bmatrix} -.006395 & -.024968 & -.081211 & -.168026 & -.245191 \\ -.002082 & -.019498 & -.074879 & -.169533 & -.270095 \\ .006751 & -.006304 & -.055046 & -.167809 & -.348428 \\ .009465 & .004410 & -.023447 & -.143234 & -.484922 \\ .000000 & .000000 & .000000 & -.079999 & -.639999 \end{bmatrix} T$$

$$(N_{xy}) = \begin{bmatrix} .000000 & .000000 & .000000 & .000000 & .000000 \\ .000000 & -.007952 & -.019160 & -.025755 & .000000 \\ .000000 & -.008864 & -.027699 & -.047132 & .000000 \\ .000000 & .000111 & -.015226 & -.050940 & .000000 \\ .000000 & .000000 & .000000 & .000000 & .000000 \end{bmatrix} T$$

Hyperbolic Paraboloid: c/h = 24

$$(w) = \begin{bmatrix} .000000 & -.009923 & -.046435 & -.100689 & -.158179 \\ .011922 & .000076 & -.038812 & -.095694 & -.153720 \\ .036101 & .023188 & -.018263 & -.079265 & -.139246 \\ .064239 & .051107 & .008492 & -.055337 & -.117062 \\ .090063 & .076175 & .033802 & -.028063 & -.090660 \end{bmatrix} \frac{Ta^2}{Eh^2}$$

$$(M_x) = \begin{bmatrix} .026462 & .035452 & .023654 & .004315 & .000000 \\ .031588 & .036057 & .023992 & .001523 & .000000 \\ .034435 & .038051 & .026067 & -.001360 & .000000 \\ .035018 & .039311 & .028285 & -.002806 & .000000 \\ .037034 & .037979 & .025991 & .000973 & .000000 \end{bmatrix} Th$$

$$(M_y) = \begin{bmatrix} -.031792 & -.026666 & -.020329 & -.013318 & -.011891 \\ -.016343 & -.017482 & -.017233 & -.015246 & -.013352 \\ -.005277 & -.006409 & -.008275 & -.009997 & -.010281 \\ .003086 & .003802 & .001927 & -.004461 & -.005623 \\ .000000 & .000000 & .000000 & .000000 & .000000 \end{bmatrix} Th$$

$$(M_{xy}) = \begin{bmatrix} .000000 & .000000 & .000000 & .000000 & .000000 \\ .000000 & -.002643 & -.003895 & -.003079 & -.001660 \\ .000000 & -.001671 & -.003558 & -.003548 & -.002466 \\ .000000 & -.000631 & -.000595 & -.001159 & -.001743 \\ .000000 & -.000341 & .001470 & .000727 & .000000 \end{bmatrix} Th$$

$$(f) = \begin{bmatrix} .002069 & .003097 & .005934 & .006621 & -.004999 \\ .001430 & .002217 & .004844 & .005854 & -.004999 \\ .000730 & .001371 & .003606 & .004806 & -.004999 \\ .000262 & .000684 & .002181 & .003161 & -.004999 \\ .000000 & .000000 & .000000 & .000000 & -.004999 \end{bmatrix} Ta^2$$

$$(N_x) = \begin{bmatrix} -.020425 & -.028154 & -.034890 & -.024560 & .000000 \\ -.001001 & .000540 & -.002359 & -.004476 & .000000 \\ .003726 & .002535 & -.002995 & -.009574 & .000000 \\ .003293 & .000057 & -.012103 & -.024247 & .000000 \\ .008387 & .021888 & .069807 & .101158 & .000000 \end{bmatrix} T$$

$$(N_y) = \begin{bmatrix} .032904 & .028941 & -.034400 & -.196939 & -.428106 \\ .025175 & .029438 & -.025867 & -.189825 & -.452666 \\ .020529 & .025493 & -.016551 & -.176116 & -.486179 \\ .013500 & .017209 & -.008284 & -.146254 & -.538841 \\ .000000 & .000000 & .000000 & -.079999 & -.639999 \end{bmatrix} T$$

$$(N_{xy}) = \begin{bmatrix} .000000 & .000000 & .000000 & .000000 & .000000 \\ .000000 & .003955 & .000355 & -.009312 & .000000 \\ .000000 & .005975 & .004637 & -.010651 & .000000 \\ .000000 & .011505 & .013741 & -.014425 & .000000 \\ .000000 & .000000 & .000000 & .000000 & .000000 \end{bmatrix} T$$

Hyperbolic Paraboloid c/h = 30

$$(w) = \begin{bmatrix} .000000 & -.014773 & -.061773 & -.129394 & -.200325 \\ .009543 & -.006290 & -.055236 & -.125478 & -.196779 \\ .030192 & .013788 & -.037126 & -.111233 & -.184315 \\ .054898 & .038604 & -.013104 & -.089991 & -.164620 \\ .077287 & .060347 & .009253 & -.065059 & -.140509 \end{bmatrix} \frac{Ta^2}{Eh^2}$$

$$(M_x) = \begin{bmatrix} .039396 & .042968 & .027493 & .004414 & .000000 \\ .042223 & .044149 & .028393 & .001413 & .000000 \\ .043745 & .046013 & .030923 & -.001367 & .000000 \\ .043449 & .047221 & .033570 & -.003009 & .000000 \\ .045174 & .045536 & .030961 & .001514 & .000000 \end{bmatrix} Th$$

$$(M_y) = \begin{bmatrix} -.025448 & -.022621 & -.017432 & -.010441 & -.009454 \\ -.014807 & -.015460 & -.015431 & -.013771 & -.011892 \\ -.005408 & -.006317 & -.007882 & -.009330 & -.009639 \\ .003089 & .004099 & .002218 & -.004918 & -.005888 \\ .000000 & .000000 & .000000 & .000000 & .000000 \end{bmatrix} Th$$

$$(M_{xy}) = \begin{bmatrix} .000000 & .000000 & .000000 & .000000 & .000000 \\ .000000 & -.001848 & -.003467 & -.002879 & -.001433 \\ .000000 & -.001074 & -.003136 & -.003324 & -.002218 \\ .000000 & -.000238 & -.000128 & -.000858 & -.001578 \\ .000000 & -.000020 & .002126 & .001168 & .000000 \end{bmatrix} Th$$

$$(f) = \begin{bmatrix} .002276 & .003196 & .005747 & .006408 & -.004999 \\ .001667 & .002354 & .004636 & .005597 & -.004999 \\ .000980 & .001555 & .003495 & .004606 & -.004999 \\ .000433 & .000851 & .002242 & .003133 & -.004999 \\ .000000 & .000000 & .000000 & .000000 & -.004999 \end{bmatrix} Ta^2$$

$$(N_x) = \begin{bmatrix} -.019497 & -.026946 & -.035556 & -.025962 & .000000 \\ -.001243 & .000694 & -.000475 & -.002870 & .000000 \\ .002239 & .001516 & -.001791 & -.007716 & .000000 \\ .001820 & -.002368 & -.015833 & -.026568 & .000000 \\ .013863 & .027263 & .071756 & .100272 & .000000 \end{bmatrix} T$$

$$(N_y) = \begin{bmatrix} .029444 & .026087 & -.030228 & -.193116 & -.434926 \\ .021995 & .025506 & -.021126 & -.184932 & -.460889 \\ .018420 & .021818 & -.013249 & -.171483 & -.492592 \\ .013399 & .015547 & -.007989 & -.144394 & -.539727 \\ .000000 & .000000 & .000000 & -.079999 & -.639999 \end{bmatrix} T$$

$$(N_{xy}) = \begin{bmatrix} .000000 & .000000 & .000000 & .000000 & .000000 \\ .000000 & .003822 & .000645 & -.009008 & .000000 \\ .000000 & .004638 & .003844 & -.009574 & .000000 \\ .000000 & .010059 & .012202 & -.013980 & .000000 \\ .000000 & .000000 & .000000 & .000000 & .000000 \end{bmatrix} T$$

Hyperbolic Paraboloid: c/h = 40

$$(w) = \begin{bmatrix} .000000 & -.019479 & -.077338 & -.159355 & -.244776 \\ .007225 & -.012562 & -.071971 & -.156680 & -.242293 \\ .023851 & .003849 & -.056853 & -.144980 & -.232206 \\ .044542 & .024954 & -.036269 & -.127249 & -.215755 \\ .062849 & .042700 & -.017615 & -.105364 & -.194649 \end{bmatrix} \frac{Ta^2}{Eh^2}$$

$$(M_x) = \begin{bmatrix} .051944 & .051173 & .032210 & .004539 & .000000 \\ .052766 & .052828 & .033732 & .001205 & .000000 \\ .053336 & .054268 & .036565 & -.001200 & .000000 \\ .052232 & .055515 & .039675 & -.003299 & .000000 \\ .053732 & .053555 & .036575 & .002050 & .000000 \end{bmatrix} Th$$

$$(M_y) = \begin{bmatrix} -.019267 & -.018444 & -.014311 & -.007133 & -.006622 \\ -.012534 & -.012660 & -.013002 & -.012033 & -.010138 \\ -.005420 & -.006257 & -.007287 & -.008040 & -.008484 \\ .003177 & .004479 & .002574 & -.005539 & -.006206 \\ .000000 & .000000 & .000000 & .000000 & .000000 \end{bmatrix} Th$$

$$(M_{xy}) = \begin{bmatrix} .000000 & .000000 & .000000 & .000000 & .000000 \\ .000000 & -.001121 & -.002984 & -.002638 & -.001203 \\ .000000 & -.000538 & -.002695 & -.003054 & -.001928 \\ .000000 & .000079 & .000255 & -.000560 & -.001372 \\ .000000 & .000230 & .002760 & .001635 & .000000 \end{bmatrix} Th$$

$$(f) = \begin{bmatrix} .002327 & .003110 & .005313 & .006030 & -.004999 \\ .001777 & .002335 & .004178 & .005154 & -.004999 \\ .001172 & .001659 & .003210 & .004258 & -.004999 \\ .000606 & .001020 & .002273 & .003071 & -.004999 \\ .000000 & .000000 & .000000 & .000000 & -.004999 \end{bmatrix} Ta^2$$

$$(N_x) = \begin{bmatrix} -.017609 & -.024811 & -.036330 & -.028033 & .000000 \\ -.000867 & .001593 & .002676 & -.000308 & .000000 \\ .000619 & .000585 & .000503 & -.004678 & .000000 \\ -.000655 & -.006097 & -.021395 & -.030135 & .000000 \\ .019416 & .032647 & .072761 & .098277 & .000000 \end{bmatrix} T$$

$$(N_y) = \begin{bmatrix} .025059 & .022722 & -.023788 & -.187947 & -.447032 \\ .017858 & .020563 & -.013880 & -.178078 & -.475066 \\ .015578 & .017026 & -.008040 & -.164917 & -.503716 \\ .013231 & .013441 & -.007298 & -.141896 & -.541722 \\ .000000 & .000000 & .000000 & -.079999 & -.639999 \end{bmatrix} T$$

$$(N_{xy}) = \begin{bmatrix} .000000 & .000000 & .000000 & .000000 & .000000 \\ .000000 & .003794 & .001281 & -.008413 & .000000 \\ .000000 & .002937 & .003072 & -.007618 & .000000 \\ .000000 & .008151 & .010397 & -.012841 & .000000 \\ .000000 & .000000 & .000000 & .000000 & .000000 \end{bmatrix} T$$

CASE 2. ALL FOUR EDGES PRESTRESSED

The forces and moments resulting from the prestressing of all four edges of the inverted umbrella under consideration may be determined by the superposition of these functions obtained for the case of two opposite edges prestressed. This will be referred to as Case 2, and is obtained by adding functional matrices determined in Case 1 as follows:

$$[M_x]_2 = [M_x]_1 + [M_x]_1' = [N_y]_2'$$
$$[N_x]_2 = [N_x]_1 + [N_x]_1' = [N_y]_2'$$
$$[M_{xy}]_2 = [M_{xy}]_1 + [M_{xy}]_1'$$
$$[N_{xy}]_2 = [N_{xy}]_1 + [N_{xy}]_1'$$

The bracketed terms are matrices and the prime symbol represents the transpose of the matrix.

Discussion of this paper is invited. Please forward your Discussion to PCI Headquarters before May 1 to permit publication in the August 1967 issue of the PCI JOURNAL.